

A Methodology for the Performance Characterisation of a Variable Speed CO₂ Compressor

L. Makaum, P.v.Z. Venter and M. van Eldik

Abstract—Heat pump cycles have a vast range of industrial applications. A refrigerant withdraws heat from a reservoir, transferring it to another fluid. In order to design and sufficiently size these cycles, accurate working predictions of all the components are crucial. Amongst this component are the compressor. Some analytical formulations do exist to predict the working parameters of a single hertz compressor. However, in most cases measurements and specifications known only by the manufacturer, or difficult to obtain are needed.

This paper provides a numerical methodology that allows empirical derivation of operating equations for a multi-hertz reciprocating compressor. Operational equations are derived for a reciprocating carbon dioxide multi-hertz compressor at 50 Hz. Three from five operating parameters must be known to calculate the remaining two. These parameters are the mass flow rate, inlet and outlet temperatures and pressures. The equations were tested against 40 additional data sets, proving accurate within 2.10%.

Keywords—Methodology, performance, variable, speed.

I. INTRODUCTION

Thermodynamic cycles are critical to everyday life in the modern age. Ranging from power generation to heating and cooling, the applications and necessity of thermodynamic cycles cannot be ignored. The vapour-compression cycle in particular is used for air conditioning, refrigeration and heat pump cycles [1]. A vapour-compression cycle uses a fluid, known as a refrigerant, to transfer thermal energy as it moves through the applicable components.

Climatologists have called for a worldwide phase-out of high global warming potential (GWP) refrigerants, referred to as the Kyoto Protocol [2]. This will have the same result as with the signing of the Montreal Protocol that phased-out high ozone depleting refrigerants in 1987, with all production of CFC's ending in 1995 [3]. This leads to a new phase of refrigerant upgrading. Substitutes for a few have already been found like R-1234yf that has all of the same properties for R-134a except for its ozone depletion potential (ODP) and GWP which is 0 and 4 respectively.

P.v.Z. Venter is with the School of Mechanical and Nuclear Engineering, North-West University, Potchefstroom, South-Africa .

L. Makaum was with School of Mechanical and Nuclear Engineering, North-West University, Potchefstroom, South-Africa (12330825@nwu.ac.za).

M. van Eldik, School of Mechanical and Nuclear Engineering, North-West University, Potchefstroom, South-Africa.

The early 1990's also brought about new growth in the heat pumps market, due to the pressures of various laws regarding the restrictions of CO₂ emissions [4]. In the application of heat pumps, a calculation tool should be used to predict behavioral aspects so that the heat pump can adapt in such a way that environmental impact is further minimised [4]. The tool mentioned should remain as mathematically simple as possible [4].

Heat pump systems are generally designed to satisfy maximum load, however, due to wide variations in load conditions, these systems operate at part load for the bigger margin of its lifetime [5]. Conventional part load conditions are normally controlled through on/off switches and to an extent, result in lower efficiencies, larger losses, poor temperature control and reduced reliability, resulting in higher maintenance costs [5]. Theoretically, the most efficient capacity control method is a variable speed control that can continuously match the compressor capacity to the load required [5].

Normally, manufacturers characterise single-stage compressors based on the Standard *EN 13771-1 (2003)* as cited by [6]. The standard delivers several procedures, which require the definition of three external parameters: evaporating and condensing pressure along with the superheat at the compressor inlet followed by measuring the mass flow rate and power consumption [6]. The addition of a variable speed drive (VSD) delivers one more parameter into these procedures, namely the operating frequency.

Controlling compressors by means of varying the rotational speed improves general performance and enables the compressor to deliver the required refrigeration capacity [7].

The Bitzer compressor used in this paper has no existing characterisation equations that can be used to predict the performance for a set of proposed operating conditions.

This paper provides a methodology to derive empirical equations for the performance of a multi-hertz reciprocating compressor. Numerical equations are developed for the typical operating range at 50 Hz.

II. LITERATURE SURVEY

Three approaches to compressor modelling were identified and investigated by [8]. The first was an exergy analysis method used with the purpose of identifying and measuring shaft power [9]. The second is a method using dimensionless compressor

parameters [10]. Lastly, a method detaching the volumetric and isentropic efficiencies was created by [8]. The last mentioned method required three types of work; that over the suction and discharge pressures, that due to under-pressure needed at suction and the work due to over-pressure at the discharge.

A model was proposed by [4] that required six variables. These variables included the swept volume, operating frequency of the motor, temperature of the inside wall, global heat transfer coefficient at suction, diameter of the suction pipe and the ratio between the dead space and swept volume.

The values needed for swept volume, diameter of the suction pipe and the ratio between the dead space and swept volumes are all obtainable from the manufacturer's data sheets. The temperature of the inside wall and global heat transfer coefficient values are not given in any information sheet. In this model the wall temperature was assumed to be constant, whilst the heat transfer coefficient was iteratively determined [4].

The authors of [11] published a model where the compressor was divided into six separate processes. These six processes are the heating of vapour at suction due to cooling effects and friction at the suction end, vapour heated due to heat transfer from the discharge side, isenthalpic pressure loss at the suction valve, isentropic compression from actual intake conditions (leakages and condensation may be present), isenthalpic pressure loss at the discharge valve and finally vapour cooling due to heat transferred from the suction side [11]. Thermodynamic equations were defined for all of these processes based on dimensions and fluid properties. This model incorporated the iterative Monte-Carlo method to determine the correct parameters [11].

In summary, these approaches are all analytical and deliver complex, iterative equations. Numerical modelling are more rare, like [7] generated models for variable speed refrigeration systems, but the assumption was made that the compressor had a constant efficiency of 70 %. This will certainly lower accuracy when compressors are varied.

Reference [12] presented a simpler modelling technique to that of [11], using the same processes but instead of iteratively determining some of the variables, the compressor was equipped with internal sensors. This model further still needed values that are difficult to determine. These values include the volumes and clearance factor, along with throttling parameters, heat transfer coefficients, parameters for shaft power and a losses term [12]. Mass flows, power consumption and exhaust temperatures are the delivered variables [12].

A map-based method was used for the modelling of an inverter compressor by [13]. The model is based upon the reasoning that a variable speed compressor at a certain frequency will perform the same as a similar, constant speed compressor at that frequency [13]. The data they obtained from performance curves was interpolated and extrapolated to deliver sensible data at other frequencies [13]. The result is an uncertain relationship between performance and frequency [13]. The modelling equations delivered were in the form;

$$M_0 = a_1 T_c^2 + a_2 T_c + a_3 T_c T_e + a_4 T_e^2 + a_5 T_e + a_6$$

$$P_0 = b_1 T_c^2 + b_2 T_c + b_3 T_c T_e + b_4 T_e^2 + b_5 T_e + b_6$$

Procedure for Paper Submission The mass flow and power output is defined by M_0 and P_0 respectively, while T_c is the condensing temperature and T_e the evaporating temperature. The constants $a_1 - a_6$ and $b_1 - b_6$ are dependent on the specific compressor.

III. METHODOLOGY

The manufacturer's software is used to obtain the data used in this study. The software can be used to simulate a variety of their compressors with the applicable refrigerant. The equipment in question is the JTC-15K reciprocating, semi-hermetic CO₂ compressor.

The variables needed for the empirical equations are the suction temperature in the form of degree of superheat (DOS) or $C(T_{in})$, suction pressure in *Bar* (P_{in}), discharge pressure in *Bar* (P_{out}), operating frequency in *Hz*, mass flow through the compressor *g/s* (\dot{m}) and the discharge temperature in *C* (T_{out}).

The first four variables mentioned are controllable, whereas the last two are results from the simulation. Note that the suction pressure follows from the saturation temperature. The mass flow is also delivered in *kg/h* but is converted to *g/s*.

The compressor's operational limits for this paper is a minimum DOS of 5 *K*, and upper temperature limit of 160 *C*, an exit pressure within the range of 75 and 110 *Bar*, and an inlet temperature between 0-20 *C*.

The method to follow is used as a test matrix to obtain data from the software provided.

1. Set fixed values for the frequency at 50 *Hz* and suction and discharge pressures at 20 and 75 *Bar* respectively. The suction saturation temperature corresponding with every pressure is given in Table I.

2. Increase the inlet temperature from the minimum allowable integer, as shown in Table I with a step of 1 *C* until either one of the limits are reached.

3. Increase the discharge pressure with a step of 5 *Bar* and repeat step 2, until the discharge pressure limit is reached.

4. Increase the suction pressure with a step of 5 *Bar* and repeat steps 2 and 3 until the upper suction pressure boundary is met.

The methodology to determine the numerical equations are based on mathematical reasoning, where:

$$\begin{aligned} T_{out} &= f(T_{in}) \\ T_{out} &= f(P_{in}) \\ T_{out} &= f(P_{out}) \end{aligned}$$

And therefore:

$$T_{out} = f(T_{in}, P_{in}, P_{out})$$

The same applies for the mass flow equations;

$$\begin{aligned} \dot{m} &= f(T_{in}) \\ \dot{m} &= f(P_{in}) \\ \dot{m} &= f(P_{out}) \end{aligned}$$

And therefore;

$$\dot{m} = f(T_{in}, P_{in}, P_{out})$$

Through application of the mentioned reasoning, a fixed methodology can be created. By keeping two of the input variables given a constant, proper correlation can be

determined. This process can be repeated, which is summarised as:

1. At a fixed frequency and suction pressure create a correlation for the temperature out vs in. Create these correlations for every discharge pressure from 75 to 110 Bar in steps of 5 Bar.
2. Using the correlations in step 1, create new correlations for the variations in slope and intercept values as a function of discharge pressure.
3. Test these correlations with data not used in their creation, but generated at random.
4. Using the correlations resulting from step 2, create a new set of correlations for the slope and intercept values as a function of suction pressure.
5. Repeat this from step 1, using mass flow instead of temperature in as the “y” coordinate.

Keep in mind that these equations may be in linear or polynomial form. Therefore, proper graphical illustration before every correlation is needed to ensure that the most suitable equation form is applied.

IV. NUMERICAL EQUATIONS

The application of the mentioned methodology result in a number of numerical equations. The 30 Bar suction pressure equations are given in Table I. Similar equations exist for 20, 25, 35 and 40 Bar.

These equations are a correlation for the predicted exit temperature as a function of the suction temperature. For each discharge pressure, there is one corresponding equation. Each inlet pressure has a set of these equations, as shown in Table I.

TABLE I:
CORRELATIONS FOR 30 BAR SUCTION PRESSURE

P_{out}	$P_{in} = 30 \text{ Bar}$	
75 Bar	$T_{out} = 1.367 \cdot T_{in} + 83$	$\dot{m} = -1.148 \cdot T_{in} + 159$
80 Bar	$T_{out} = 1.397 \cdot T_{in} + 90$	$\dot{m} = -1.122 \cdot T_{in} + 155$
85 Bar	$T_{out} = 1.425 \cdot T_{in} + 96$	$\dot{m} = -1.099 \cdot T_{in} + 152$
90 Bar	$T_{out} = 1.456 \cdot T_{in} + 102$	$\dot{m} = -1.075 \cdot T_{in} + 149$
95 Bar	$T_{out} = 1.484 \cdot T_{in} + 109$	$\dot{m} = -1.053 \cdot T_{in} + 146$
100 Bar	$T_{out} = 1.515 \cdot T_{in} + 114$	$\dot{m} = -1.021 \cdot T_{in} + 142$
105 Bar	$T_{out} = 1.543 \cdot T_{in} + 120$	$\dot{m} = -1.009 \cdot T_{in} + 139$
110 Bar	$T_{out} = 1.575 \cdot T_{in} + 126$	$\dot{m} = -0.986 \cdot T_{in} + 137$

The data is plotted graphically in Fig. 1. It is clear that the correlations for 30 Bar suction pressure are all sufficiently accurate in linear form. This is also the case for the other suction pressures.

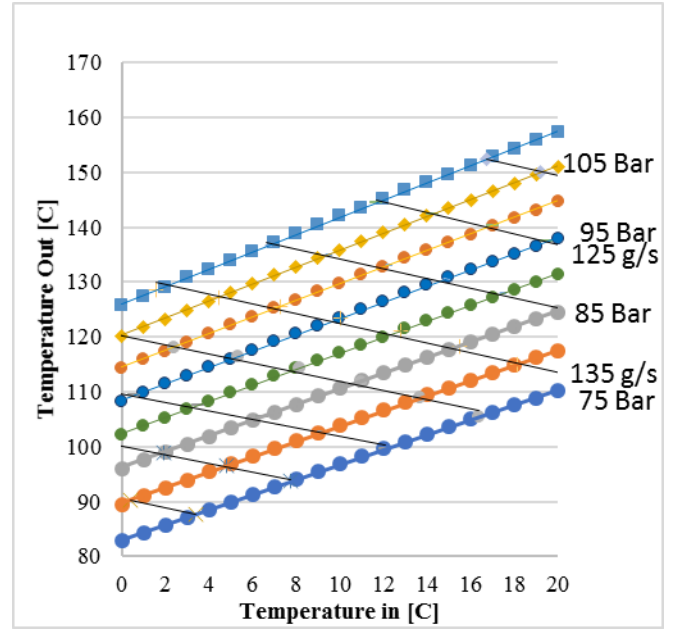


Fig. 1: Data for 30 Bar Plotted Graphically

By holding the coefficient values in large decimal numbers, a small insignificant increase in accuracy is obtained. Further processing on these equations are done with the unrounded numbers, since the value when referenced into another equation is the real value with all decimal numbers included.

Step 2 in the equation creation methodology delivers the numerical equations given in Table I. In the Fig. 2, the inlet temperature slope values for the mass flows of the equation sets in Table I are plotted over the corresponding discharge pressures. A linear relationship follows with a R^2 value close to unity.

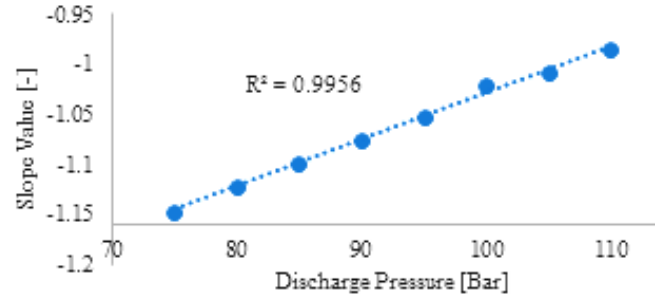


Fig. 2: Slope Variations for \dot{m} Equation @ 30 Bar Suction

This step is repeated for the mass flow intercepts, as well as the outlet temperature’s gradients and intercepts. Linear correlations follow for both the slopes and intercepts graphs. The correlations, similar to that shown in Fig. 2, have their own equations. Since these correlations were for the slope and intercept values as a function of discharge pressures, the slopes and intercepts of the equations in Table I can be replaced by these correlations. The resulting equations are given in Table II.

TABLE II:
EQUATIONS AFTER CORRELATIONS FOR DISCHARGE TEMPERATURE

P_{in} [Bar]	
20	$T_{out} = (0.01 \cdot P_{out} + 0.73) \cdot T_{in} + (1.68 \cdot P_{out} + 10.72)$ $\dot{m} = (-0.002 \cdot P_{out} - 0.34) \cdot T_{in} + (-0.5 \cdot P_{out} + 117.7)$
25	$T_{out} = (0.07 \cdot P_{out} + 0.83) \cdot T_{in} + (1.37 \cdot P_{out} + 3.31)$ $\dot{m} = (-0.0007 \cdot P_{out} - 0.63) \cdot T_{in} + (-0.52 \cdot P_{out} + 155.4)$
30	$T_{out} = (0.006 \cdot P_{out} + 0.92) \cdot T_{in} + (1.23 \cdot P_{out} - 8.25)$ $\dot{m} = (0.005 \cdot P_{out} - 1.5) \cdot T_{in} + (-0.64 \cdot P_{out} + 206.5)$
35	$T_{out} = (0.006 \cdot P_{out} + 0.90) \cdot T_{in} + (1.11 \cdot P_{out} - 16.80)$ $\dot{m} = (0.006 \cdot P_{out} - 2.11) \cdot T_{in} + (-0.75 \cdot P_{out} + 262.9)$
40	$T_{out} = (0.006 \cdot P_{out} + 0.87) \cdot T_{in} + (1.02 \cdot P_{out} - 23.60)$ $\dot{m} = (0.007 \cdot P_{out} - 2.71) \cdot T_{in} + (-0.86 \cdot P_{out} + 326.9)$

According to step 4, the equations are again correlated, as illustrated in Fig. 3 and 4. The slope and intercept values of each individual correlation is shown as a function of the suction pressure. The R^2 value is given to illustrate the accuracy of the correlations.

Similar illustrations to Fig.3 and 4 are created for all slope and intercept variations. This is done for both T_{out} and \dot{m} equations.

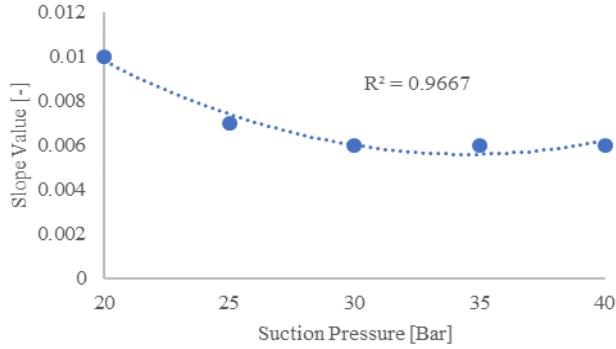


Fig. 3: Slope Variation in M1 for Tout Equation

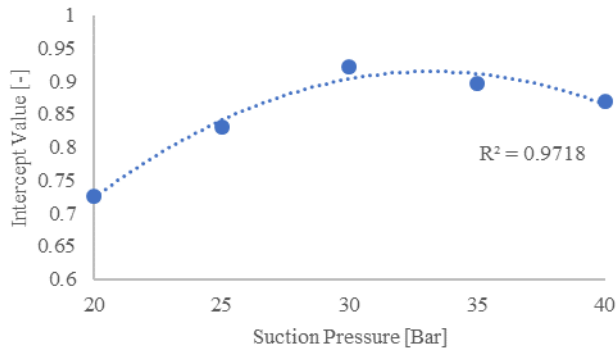


Fig. 4: Intercept Variation in C1 for Tout Equation

The correlations created in step 4, shown in Fig.3 and 4 are in quadratic form. These correlations are the last equations needed for the final predictive calculations.

Should the correlation have a sufficiently high coefficient in linear form, then the linear equation will be used since higher polynomial equations add more to the complexity of the final equations.

The final equations are then created. By again replacing the slope and intercept values of the equations given in Table II with this set of correlations, the final equations are generated.

Fig. 5 also shows the makeup of the final equations in detail.

$$T_{out} = ((2e^{-5} \cdot P_{in}^2 - 0.00138 \cdot P_{in} + 0.0294) \cdot P_{out} + (-0.00110 \cdot P_{in}^2 + 0.0729 \cdot P_{in} - 0.296)) \cdot T_{in} + (0.00134 \cdot P_{in}^2 - 0.112 \cdot P_{in} + 3.378) \cdot P_{out} - 1.775 \cdot P_{in} + 46.318 \quad [1]$$

$$\dot{m} = ((-0.000012 \cdot P_{in}^2 + 0.00124 \cdot P_{in} - 0.0224) \cdot P_{out} + (-0.00110 \cdot P_{in}^2 - 0.0586 \cdot P_{in} + 1.341)) \cdot T_{in} + (-0.00049 \cdot P_{in}^2 + 0.0104 \cdot P_{in} - 0.500) \cdot P_{out} + 0.166 \cdot P_{in}^2 + 0.588 \cdot P_{in} + 38.989 \quad [2]$$

Equations [1] and [2] are now a result of the methodology and can be used at an operating frequency of 50 Hz to determine any two operational parameters, if the other three are known. The five parameters are:

1. Mass flow rate.
2. Inlet temperature.
3. Outlet temperature.
4. Inlet pressure.
5. Outlet pressure.

V. RESULTS AND VERIFICATION

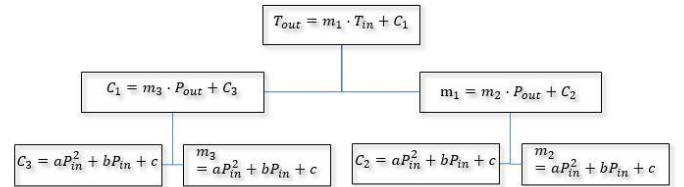


Fig. 5: Final Equation Makeup If Linear Correlations Apply to All

Fig. 5 displays the general makeup of the final equations if all correlations were found to be sufficiently accurate in linear form.

The first and second tier of equations depicted in Fig. 5 are all of linear form. The third tier, however, is in polynomial form.

Proper investigation of Fig. will lead to the understanding of how the equations fit together. In summary, the coefficients in the equations are correlated to be a function of another variable. By repeating this again for the coefficients to follow, more and more variables are included into one singular equation.

A. Testing Method

To do interim and final evaluation of the predictions, a proper testing method is required. This will ensure that accuracies obtained are both reliable and applicable.

The following method is used:

1. Generate random integers between 0 and 20 C for the T_{in} variable.
2. Create random integers between 75 and 110 Bar. These integers do not include those used for the creation of the equations. The randomised values can, for example, be 77 or 89 Bar but may not be dividable by 5 and must lie between 75 to 90 Bar.
3. If final testing is done, create another random set of integers between 20 and 40 Bar. The same conditions as in

step 2 still apply. If only interim testing is done, step 3 may be ignored.

Note that the integers in step 1-3 are not in steps, such as with the testing methodology where the discharge pressure ranges from 75 to 110 Bar in steps of 5 Bar. The discharge pressure may now be values such as 77 or 89 Bar.

The number of randomised values need to be large enough to ensure proper reliability of the outcome. A set of 30-40 values are deemed sufficient.

4. Using the integers created in steps 1-3, predict the mass flow and outlet temperature conditions.
5. If these output values exceeds the outlet temperature limit, alter one or more of the input values until the limits are not breached. This generally occurs when a relatively small suction pressure combines with a relatively high discharge pressure.
6. Determine the percentage errors on these equations along with a graphical illustration of the calculated vs. simulated values.

B. Prediction Accuracy

The final equations' respective accuracies are delivered in Table III. Fig. 6 and 7 shows the comparison graphically with the $x = y$ line again being the line where 100% accuracy is achieved.

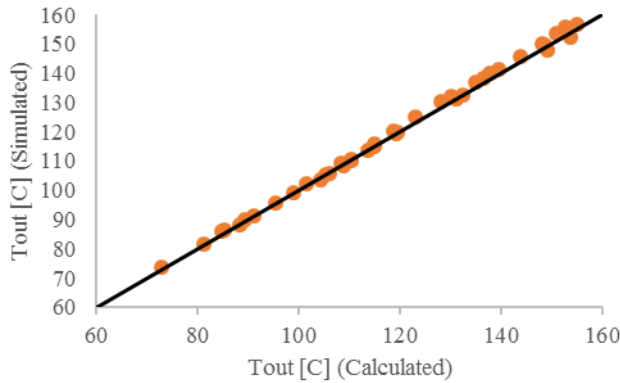


Fig. 6: Comparison between Calculated and Simulated Values for the Temperature out Equation

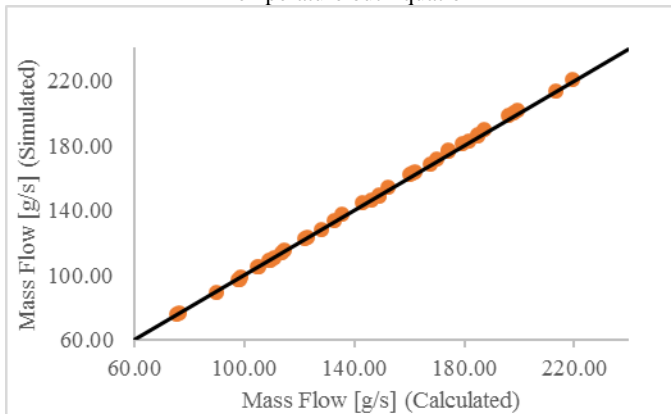


Fig. 7: Comparison between Calculated and Simulated Values for the Mass Flow Equation

TABLE III:
FINAL EQUATION ACCURACY

Type	T _{out} % Error	\dot{m} % Error
Max	2.09%	1.51%
Average	0.86%	0.66%

VI. CONCLUSION AND FURTHER RESEARCH

This paper discussed a numerical methodology that can be followed in order to determine a multi-hertz reciprocating compressor's operating parameters. A single operating hertz was chosen from where the methodology was explained how numerical equations can be determined from experimental results. There are five operating parameters that must be known to fully describe the working conditions of a compressor. These parameters and the mass flow rate, inlet, as well as the outlet temperatures and pressures. Two equations can numerically be derived and used to determine any two of the mentioned parameters if the other three are known. A carbon dioxide multi-hertz reciprocating compressor was used to demonstrate the methodology. The two working equations derived from the process were tested against 40 operational values, where none of these values were used in the derivation of the equations. The maximum error during the tests was just below 2.1%.

A sixth parameter, the hertz, was held constant. For further research, the authors are expanding the test matrix by incorporating other operational frequencies. Once this method has been expanded to all operational frequencies, it will be possible to incorporate numerical equations to predict any outcome of this multi-hertz reciprocating compressor.

REFERENCES

- [1] C. Borgnakke and R. E. Sonntag, Fundamentals of Thermodynamics, 7th SI ed., Michigan: John Wiley & Sons, 2009.
- [2] J. Calm, "The next generation of refrigerants - Historical reviews, considerations, and outlook," International Journal of Refrigeration, no. 31, pp. 1123-1133, 2008.
- [3] J. M. Calm and D. D. A., "Trade-offs in refrigerant selections: past, present and future," International Journal of Refrigeration, vol. 21, no. 4, pp. 308-321, 1998.
- [4] M. Duprez, E. Dumont and M. Frere, "Modelling of reciprocating and scroll compressors," International Journal of Refrigeration, vol. 1, no. 30, pp. 873-886, 2007.
- [5] S. Tassou and T. Quresh, "Comparative performance evaluation of positive displacement compressors in variable-speed refrigeration applications," International Journal of Refrigeration, vol. 21, no. 1, pp. 29-41, 1998.
- [6] F. Tello-Oquendo, E. Navarro-Peris and J. Gonzalves-Macia, "New characterization methodology for vapor-injection scroll compressors," International journal of refrigeration, no. 74, pp. 528-539, 2017.
- [7] R. Koury, L. Machado and K. Ismail, "Numerical simulation of a variable speed refrigeration system," International Journal of Refrigeration, vol. I, no. 24, pp. 192-200, 2001.
- [8] C. Perez-Segarra, J. Rigola, M. Soria and A. Oliva, "Detailed thermodynamic characterization of hermetic reciprocating compressors," International Journal of Refrigeration, vol. 28, no. 1, pp. 579-593, 2005.
- [9] J. McGovern and S. Harte, "An exergy method for compressor performance analysis," International Journal of Refrigeration, no. 18, pp. 421-433, 1995.
- [10] P. Stouffs, M. Tazerout and P. Wauters, "Thermodynamic analysis of reciprocating compressors," International Journal of Thermal Science, no. 40, pp. 52-66, 2001.
- [11] E. Navarro, E. Granryd, J. Urchueguia and J. Corberan, "A phenomenological model for analyzing reciprocating compressors,"

International Journal of Refrigeration, vol. I, no. 30, pp. 1254-1265, 2007.

- [12] E. Winandy, C. Saavedra and J. Lebrun, "Simplified modelling of an open-type reciprocating compressor," International Journal of Thermal Sciences, vol. I, no. 41, pp. 183-192, 2002.
- [13] S. Shao, W. Shi, X. Li and H. Chen, "Performance representation of variable-speed compressor for inverter air conditioners based on experimental data," International Journal of Refrigeration, vol. I, no. 27, pp. 805-815, 2004.